Sparse Q-compensation in the time domain with the hyperbolic penalty function

Antoine Guitton[1] and Jon Claerbout[2]
[1] *Center for Wave Phenomena, Colorado School of Mines, Golden, Colorado, USA*
[2] *Stanford Exploration Project, Stanford, California, USA*

ABSTRACT
We adopt a simple time-dependent Q model where the spectrum deplets by the amount $e^{-|\omega|t/Q}$. From this spectrum, a Futterman wavelet is estimated at each time sample by spectral factorization. We form a matrix of these wavelets to build a constant Q attenuation model. We invert these matrices to remove the effect of Q on synthetic and field data sets. To stabilize the inversion, we add a sparseness constraint using the hyperbolic penalty function, thus yielding spiky Q-compensated reflectivity series. Without the constraint, the inversion usually fails to recover any useful information.

Key words: Q, Futterman, time, inversion, sparse, hyperbolic penalty function

1 INTRODUCTION

Attenuation in the Earth is a time variant process where the spectrum is depleted by the amount $e^{-|\omega|t/Q}$ where Q is a material property. The causal response shape with spectrum $e^{-|\omega|t/Q}$ is called the Futterman wavelet and can be estimated efficiently with the Kolmogoroff spectral factorization method. This wavelet changes slowly with time and is a function of Q.

Contrary to the standard deconvolution process, the Futterman wavelet varies in time and depends only, to first order, on the propagation time in the Earth. Our goal in this paper is to undo the effect of attenuation using the Futterman wavelet as our basis function. We make two important assumptions: Q is known and Q is constant. For non-constant Q, our method can be applied if a Q(t) is known (t is recording time). To estimate Q, standard methods based on spectral ratios can be used. Alternatively and assuming a constant Q, one can run many Q-compensation processes with different Q values and pick the best number.

If the spectrum diminishes with $e^{-|\omega|t/Q}$, then the inverse will grow back by $e^{+|\omega|t/Q}$ and can easily blow up. Because inverting for the Futterman wavelet might become unstable where the spectrum is small, we add a regularization term enforcing spikiness in the final model. This regularization term stabilizes the inversion.

For the inversion, we first build what we call a Futterman matrix which takes a model space function of traveltime depth to a data space function of time. It is a square matrix with a Futterman wavelet on each row and represents the non-stationary convolution process. Having the Futterman matrix, we move on to the inversion using the hyperbolic penalty function for both data fit and model regularization terms. The hyperbolic penalty norm is a hybrid ℓ^1/ℓ^2 functional that can be minimized efficiently with a conjugate direction solver. Here, we tune the hyperbolic penalty function to work like ℓ^2 for the data fit and like ℓ^1 for the regularization to enforce spiky models.

In the processing workflow, the Q-compensation process presented here would be applied after source deconvolution. If Q is not too large and varies slowly, the deconvolution could be used after Q-compensation instead. It is not the goal of this paper to explore this possibility.

We start our paper with a quick presentation of the Futterman wavelet and its computation. We also present the Futterman matrix. Then, we detail our inversion strategy to recover the reflectivity of the model. Then, we illustrate our method on 1D time series of spikes for different Q values, different noise levels, and different Q values in the forward and backward models (testing the effect of wrong Q values on the inversion). In all but the most extreme cases of noise or Q values, our algorithm recovers the reflectivity series very well. Finally, we illustrate our method on one near-offset section from offshore Brazil and one from the continental shelf, offshore Australia.

2 MEET THE FUTTERMAN WAVELET

The attenuation model behind the Futterman wavelet is that the spectrum decreases as $e^{-|\omega|t/Q}$, where t is the propagation time. Having this spectrum, we can extract a minimum-phase wavelet. This wavelet is the Futterman wavelet and the estimation process is called Kolmogoroff spectral factorization. We illustrate in Figure 1 this process: starting from a spectrum on

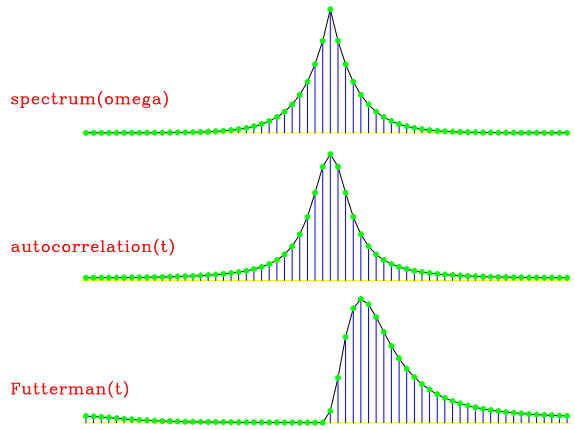

Figure 1. Top: spectrum of the Futterman wavelet. Middle: autocorrelation of the Futterman wavelet. Bottom: Futterman wavelet. The process from top to bottom is called Kolmogoroff spectral factorization.

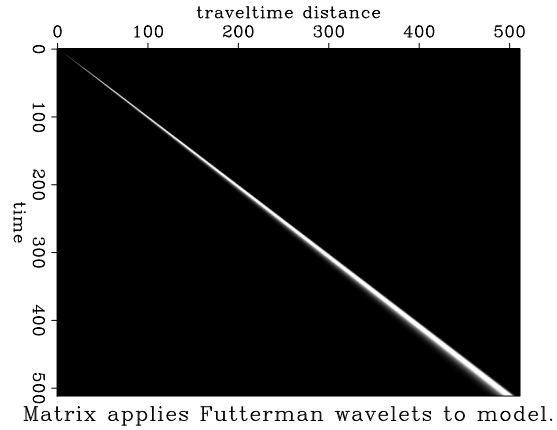

Figure 2. Futterman matrix for Q=40 and 512 time samples. On each row, a time-reversed Futterman wavelet is present. Notice how the wavelet broadens with time attenuating more and more frequencies, as expected from the Futterman model. This matrix is an attenuation operator $\mathbf{F_Q}$ that we want to invert.

top, we end up with a minimum-phase wavelet at the bottom, i.e., a Futterman wavelet.

Because the spectrum $e^{-|\omega|t/Q}$ is a function of t, a wavelet has to be estimated for each time sample. Figure 2 displays a Futterman matrix for 512 time samples and Q=40. Each row contains a time-reversed Futterman wavelet whose shape is a function of t. This matrix describes the full attenuation process: it is a non-stationary convolution operator. We call this operator $\mathbf{F_Q}$ and our goal is to undo $\mathbf{F_Q}$ assuming that Q is known and Q is constant. For a more efficient computation of $\mathbf{F_Q}$, note that for a constant Q, the Futterman wavelet at any time can be obtained by successive convolutions of a single wavelet with spectrum $e^{-|\omega|\delta t/Q}$ (Hale, 1981).

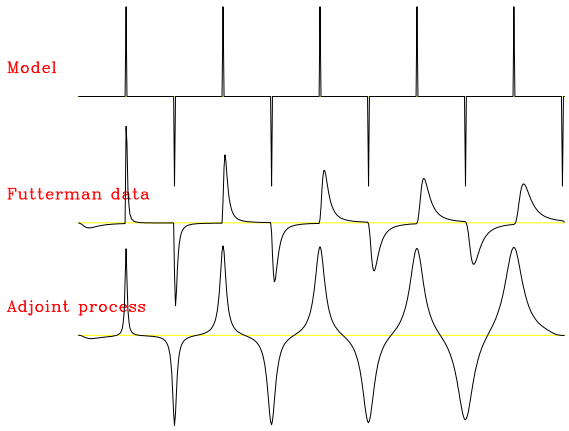

Figure 3. Top: earth model $\mathbf{m}$. Middle: data $\mathbf{F_Q m}$. Bottom: Adjoint process $\mathbf{F'_Q F_Q m}$. Applying the adjoint corrects for the phase and amplitude errors but squares the spectrum, resulting in wide blobs.

3 INVERSION OF THE FUTTERMAN MATRIX

Our attenuation model is as follows. Given an earth model in time $\mathbf{m}$ with several spaced layers, we synthesize attenuated data $\mathbf{d}$ such that

$$\mathbf{d} = \mathbf{F_Q m} \tag{1}$$

where $\mathbf{F_Q}$ is a Futterman matrix for a given Q. Figure 3 shows on top an earth model $\mathbf{m}$, in the middle the corresponding data $\mathbf{d}$, and on the bottom the adjoint process only $\mathbf{F'_Q d}$ for Q=40 and 512 time samples. We clearly see the attenuation effect increasing with time. We also notice a slight time shift. Applying the adjoint of $\mathbf{F_q}$ on $\mathbf{d}$ has the beneficial effect of centering the picks at the right location, compensating for amplitude losses, but with a broadening effect on the spectrum (we square it). For better results, inversion is needed.

3.1 Sparse inversion with the hyperbolic penalty function

Because Q-compensation would be applied after deconvolution, it makes sense to make sure that the estimated model is sparse and spiky (i.e., reflectivity). A possible cost function $\mathcal{F}(\mathbf{m})$ for such a goal becomes:

$$\mathcal{F}(\mathbf{m}) = \|\mathbf{F_Q m} - \mathbf{d}\|_2^2 + \epsilon|\mathbf{m}|_{L1}, \tag{2}$$

where we combine the ℓ^2 norm for the data fit part, and the ℓ^1 norm for the model regularization.

Minimizing such functions is complex because the ℓ^1 norm has a singularity at zero. In this paper, we use the hyperbolic penalty function

$$h(r) = \sqrt{1 + (gr)^2} - 1 \tag{3}$$

instead, where r is the residual and g a scaling factor that controls the ℓ^1/ℓ^2 behavior. A scale-free hyperbolic penalty function introducing $q = gr$ becomes

$$\bar{h}(q) = \sqrt{1 + q^2} - 1 \tag{4}$$

Using this hyperbolic penalty function, we have a new cost function $\mathcal{F}_{\bar{h}}(\mathbf{m})$ such that

$$\mathcal{F}_{\bar{h}}(\mathbf{m}) = \bar{h}(\mathbf{G_d}(\mathbf{F_Q}\mathbf{m} - \mathbf{d})) + \epsilon\bar{h}(\mathbf{G_m}\mathbf{m}), \qquad (5)$$

where $\mathbf{G_d}$ and $\mathbf{G_m}$ are scaling (diagonal) operators controlling the ℓ^1/ℓ^2 thresholds. Claerbout and Fomel (2014) show how to minimize the hyperbolic penalty function efficiently with a conjugate direction schemes.

3.2 Parameterization

In equation (5), ϵ, $\mathbf{G_d}$ and $\mathbf{G_m}$ need to be estimated. In practice, ϵ is estimated by trial and error. $\mathbf{G_d}$ and $\mathbf{G_m}$ are constant along the diagonal (but don't have to). For $\mathbf{G_d}$, the diagonal is equal to the maximum value of $\mathbf{d}$, which yields a mostly ℓ^2 treatment of the data residual. For $\mathbf{G_m}$, we pick 1% of the maximum expected value of $\mathbf{m}$, which yields a mostly ℓ^1 behavior.

In the next section we present synthetic examples of sparse inversion with different Q values, different noise levels, and inconsistent modeling and inversion Q values.

4 SYNTHETIC EXAMPLES

We test the modeling and inversion of attenuation with the Futterman wavelets using a simple reflectivity series of spikes of equal amplitude (first row of Figure 4(a), for instance). All spikes have an amplitude of 1. For all sparse inversion examples with this synthetic data, we set $\mathbf{G_d} = \mathbf{I}$ (g=1), $\mathbf{G_m} = 0.01\mathbf{I}$ (g=0.01) and $\epsilon = 0.0001$.

Each panel displayed in the following figures contains 5 rows (traces). The first row is the exact model to retrieve. The second row is the modeled data used for the inversion. The third row is the result of applying the adjoint operator only. The fourth row shows the inversion result without regularization ($\epsilon = 0$). Finally, the fifth row displays the sparse inversion result.

Figures 4(a), 4(b), 4(c), 4(d) show the processing results for Q=20, Q=40, Q=80 and Q=120, respectively. For low Q values, the adjoint process is not able to identify all the spikes. The inversion without regularization does well for high Q values (80 and 120) recovering all the spikes while failing for low Q values (20 and 40). The sparse inversion yields clean reflectivity series with accurate spikes location. As expected, all methods perform better with increasing Q values, with the sparse inversion being the most effective.

4.1 Inversion results with noisy data

The previous results were for noise free data. We now add Gaussian random noise to the modeled data. Figures 5(a), 5(b), 5(c), 5(d) show the Q compensation results when the noise variance is $\sigma^2 = 10^{-5}$. Figures 6(a), 6(b), 6(c), 6(d) show the Q compensation results when the noise variance is $\sigma^2 = 10^{-4}$. The inversion without regularization is the most affected by the noise level present in the data where the Q-compensated traces are extremely noisy for all Q values. Conversely, the sparse inversion results show robustness to the noise present in the data and yields accurate results. We seem to reach the limits of the sparse inversion approach for Q=20 and $\sigma^2 = 10^{-4}$.

4.2 Inversion with Q errors

In the next results, we model the data with a Q_{mod} value but use a different Q_{inv} for the inversion and adjoint processes. Our goal is to simulate the effect of attenuation compensation with the wrong Q value. Figures 7(a), 7(b), 7(c), 7(d), show the Q compensation results when a 20% error exists between Q_{mod} and Q_{inv}. Figures 8(a), 8(b), 8(c), 8(d), show the Q compensation results when a 40% error exists between Q_{mod} and Q_{inv}. In all cases, the sparse inversion yields sparse results. For the strong 40% error and lowest Q_{mod}, the sparse inversion gives two events in the estimated model at late time for each spike in the true model. For larger Q values, the sparse inversion recovers all the events with a time shift increasing with propagation time. Without regularization, the inversion doesn't work very well and gives noisy results.

In the next section, we show Q compensation results on field data examples.

5 FIELD DATA EXAMPLES

We apply Q-compensation to two near-offset sections from offshore Brazil and Australia. Our processing sequence is as follows:

- Sparse deconvolution in the lag-log domain
- Geometrical spreading correction
- Picking of water bottom
- Time-shifting of traces to a flat datum according to water-bottom picks
- Q-compensation
- Time-shifting back to original datum

Because attenuation only happens below the water-bottom, we first pick and shift traces so that the water-bottom appears flat. For the first break picking, we use the modified Coppens scheme of Sabbione and Velis (2010). Then, our Q-compensation scheme is applied to the time-shifted traces starting at the flattened water-bottom. This step makes it easy to quickly process all the traces in a given dataset. For both datasets, a Q value of 80 is chosen. Because the Q compensation is relatively cheap and because we assume Q to be constant, scanning over a range of Q and picking the best output could be done.

First, we show in Figure 9(a) the input data for the Brazilian dataset (with geometrical correction.) After sparse deconvolution, we obtain Figure 9(b). Having a wavelet-free dataset, we show in Figures 9(d) and 9(c) the results of attenuation compensation with and without sparse regularization, respectively. Similar to what was observed with synthetic

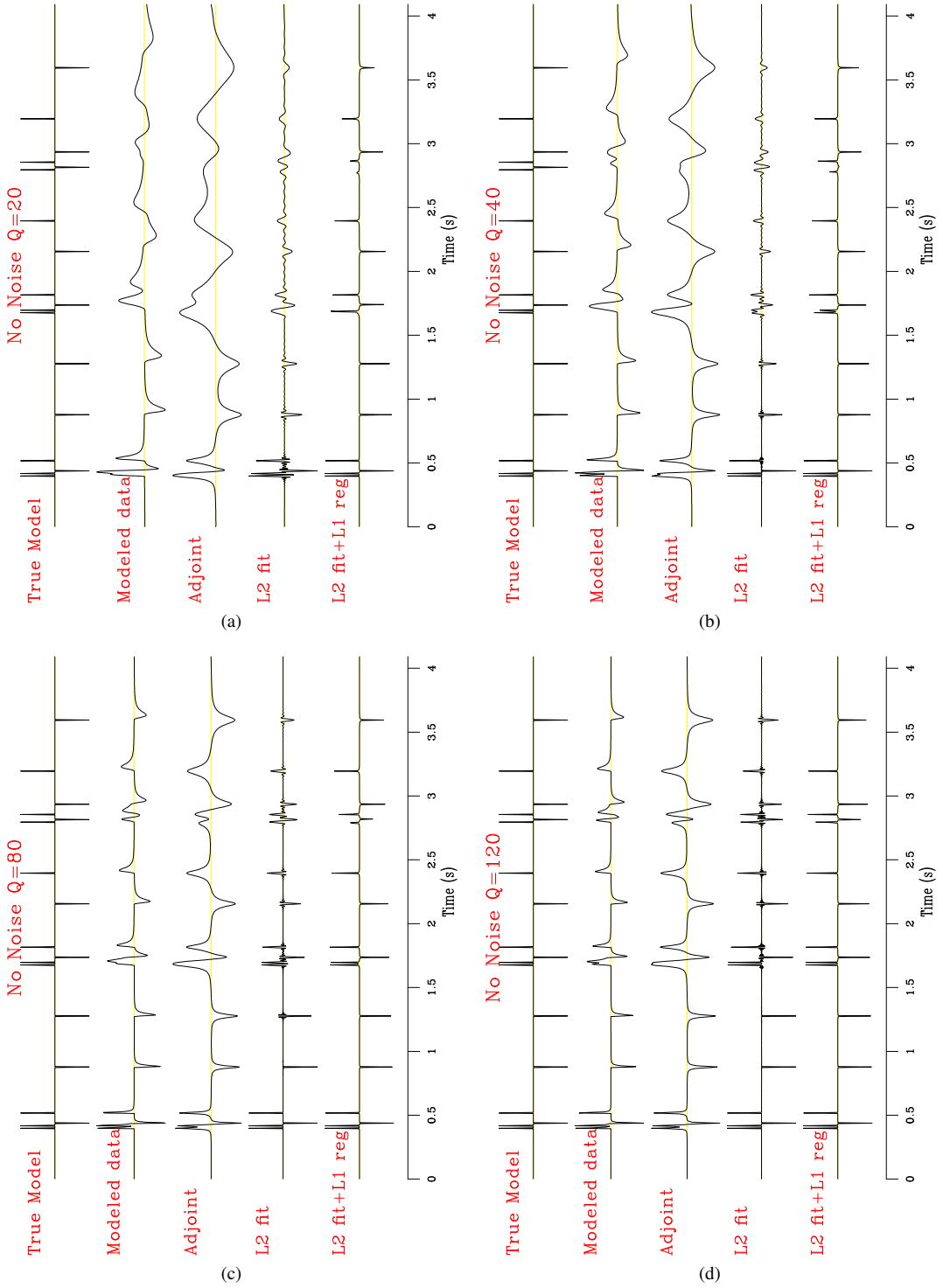

Figure 4. Q compensation results for (a) Q=20, (b) Q=40, (c) Q=80, (d) Q=120. For each panel, the first row is the true model $\mathbf{m_{true}}$, the second row the input data $\mathbf{d} = \mathbf{F_Q m_{true}}$, the third row the adjoint process $\mathbf{F'_Q d}$, the fourth row the inversion result without regularization, the fifth row the inversion result with sparse regularization.

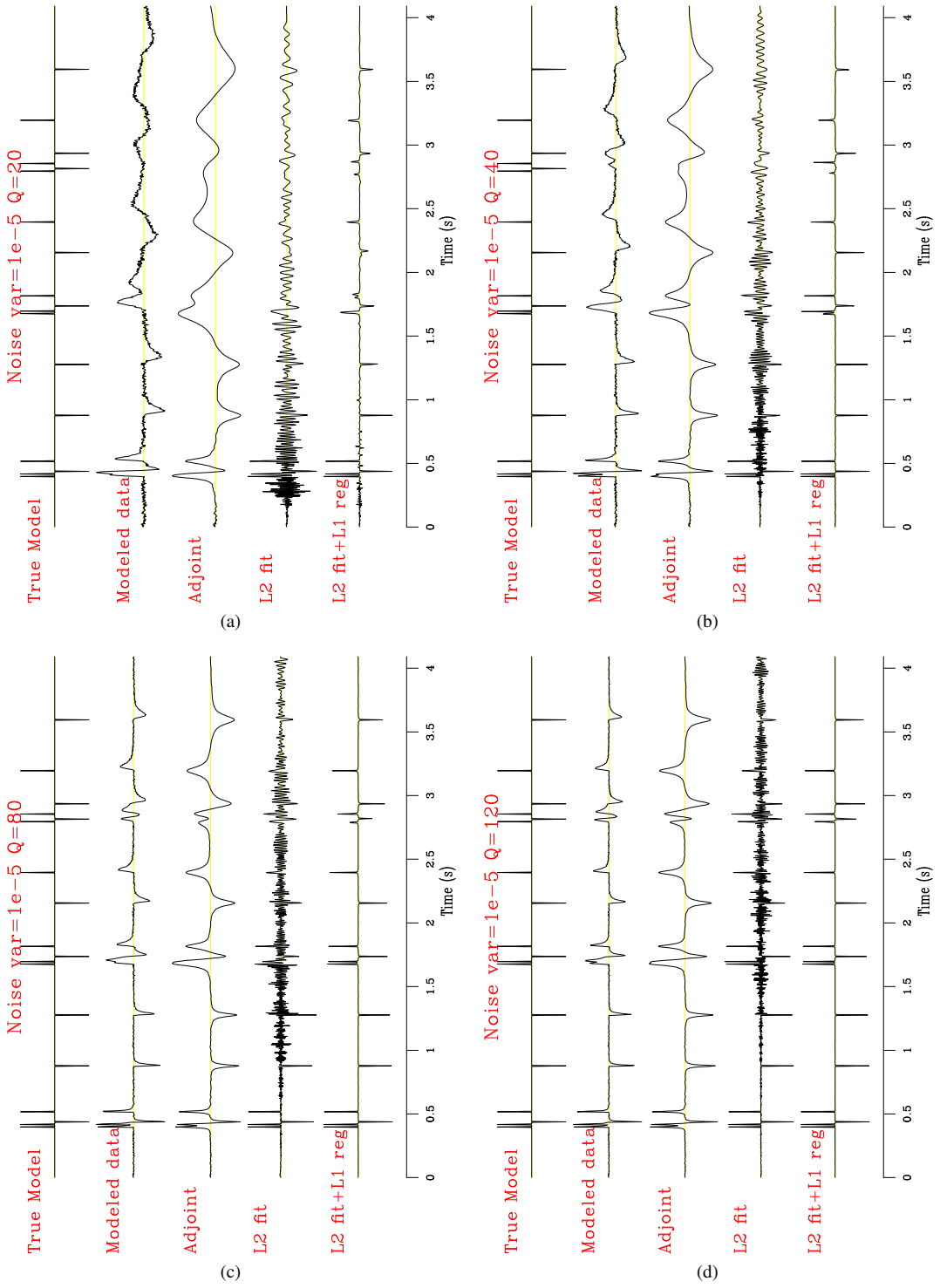

Figure 5. Q compensation results for (a) Q=20, (b) Q=40, (c) Q=80, (d) Q=120 but with random Gaussian noise with variance $\sigma^2 = 10^{-5}$ added to the data.

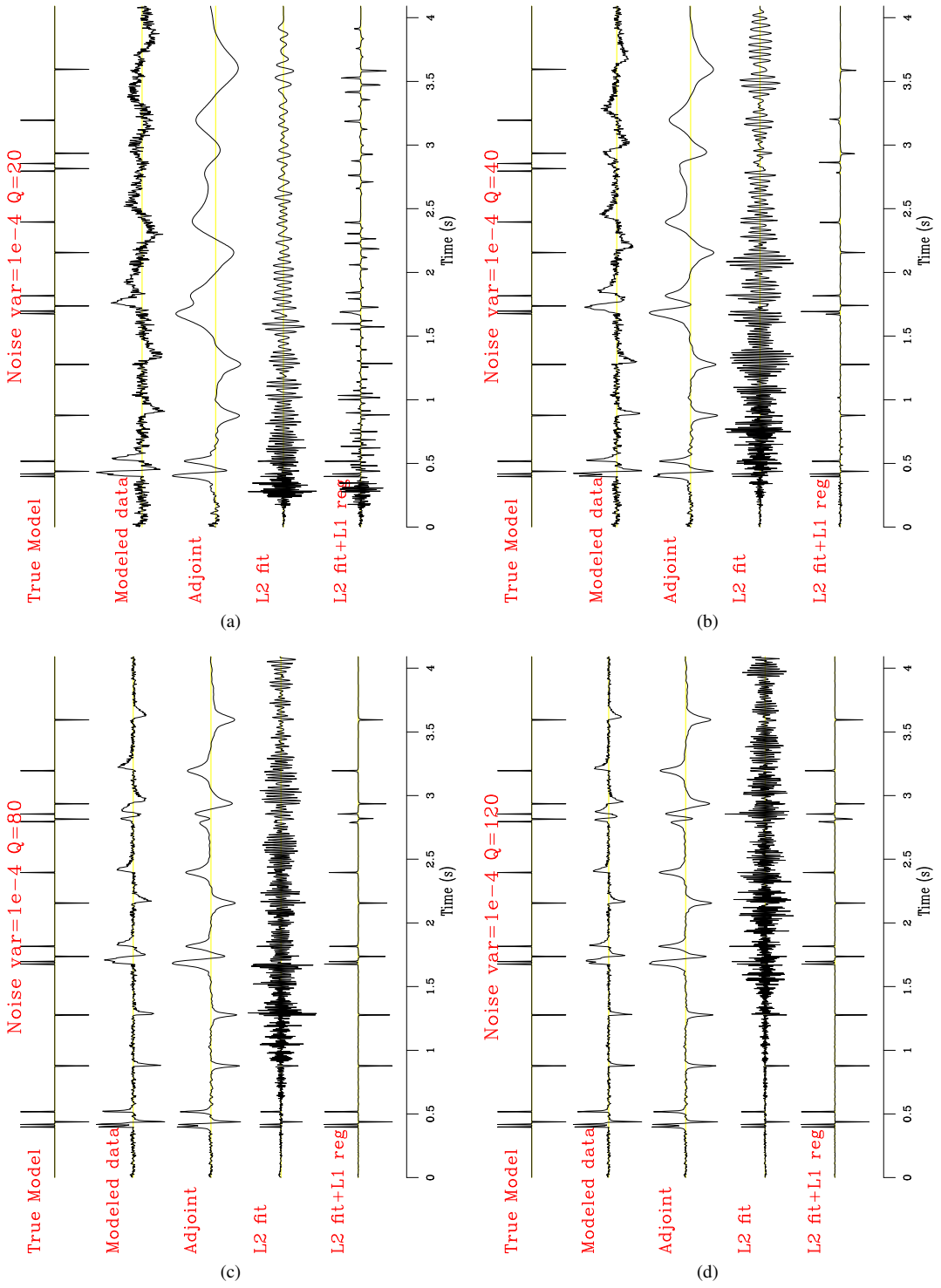

Figure 6. Q compensation results for (a) Q=20, (b) Q=40, (c) Q=80, (d) Q=120 but with random Gaussian noise with variance $\sigma^2 = 10^{-4}$ added to the data.

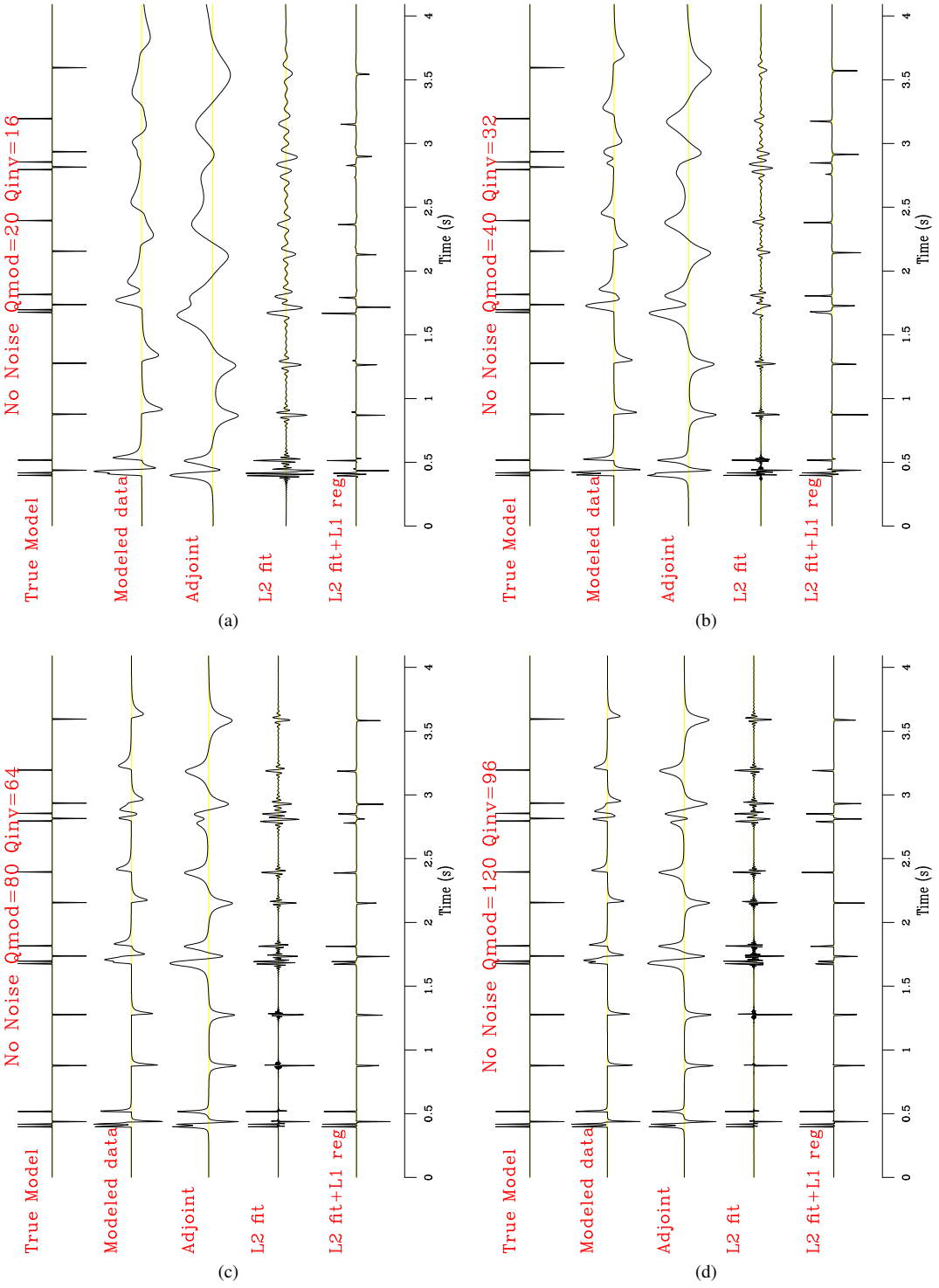

Figure 7. Q compensation results when the Q value used to invert the data (Q_{inv}) is 20% lower than the Q value (Q_{mod}) used to model the data for (a) $Q_{mod} = 20$, (b) $Q_{mod} = 40$, (c) $Q_{mod} = 80$, (d) $Q_{mod} = 120$.

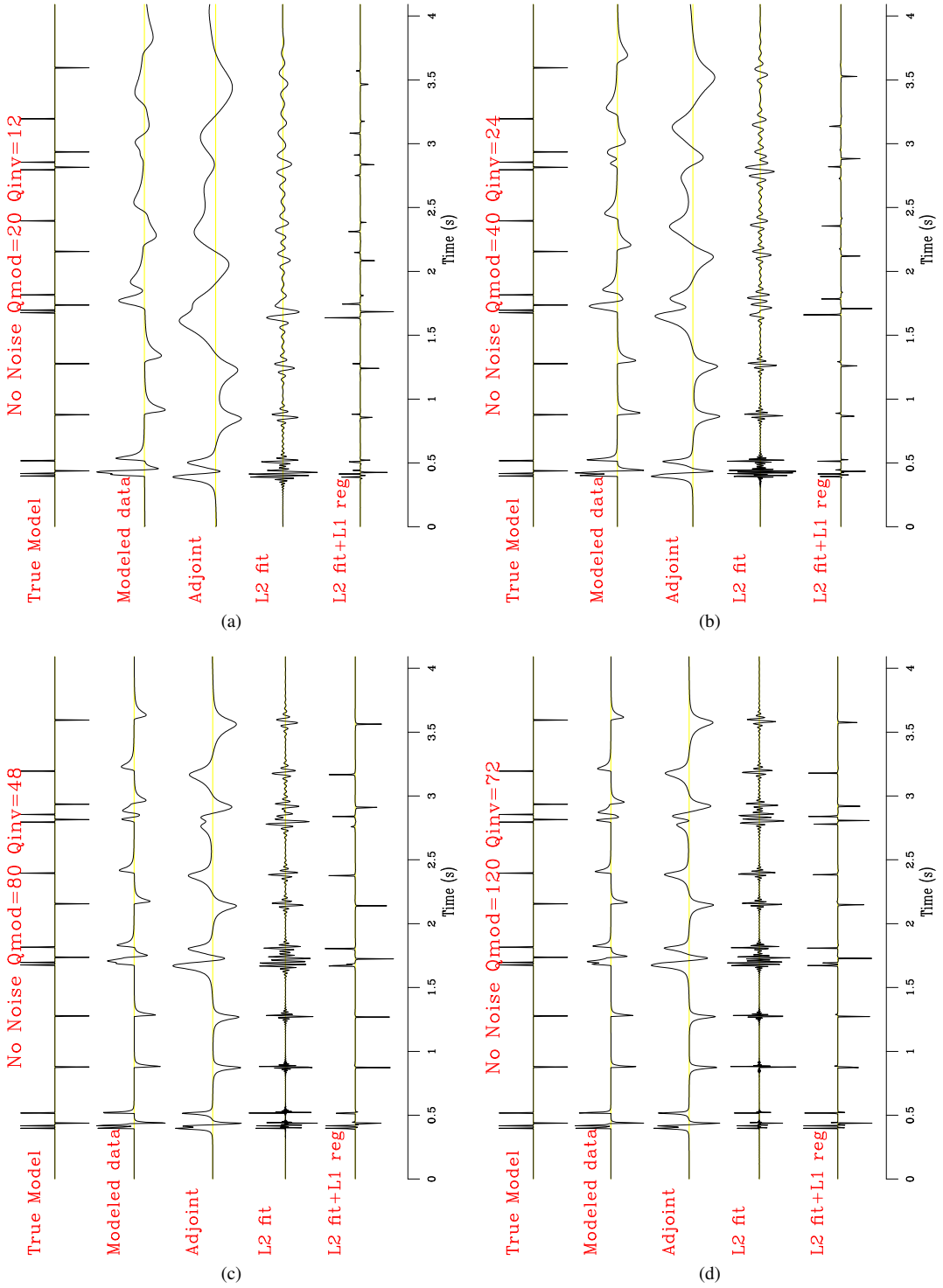

Figure 8. Q compensation results when the Q value used to invert the data (Q_{inv}) is 40% lower than the Q value (Q_{mod}) used to model the data for (a) $Q_{mod} = 20$, (b) $Q_{mod} = 40$, (c) $Q_{mod} = 80$, (d) $Q_{mod} = 120$.

data, the sparse regularization yields clean and meaningful results, while the inversion with regularization boosts high frequency noise at late times. The amplitude spectra for all four panels are shown in Figure 11(a). The most unusual behavior comes from the spectrum of the Q-compensated data using the inversion without regularization: a strong pick at 60 Hz appears, corresponding to a spectral low in the input data. Without regularization, the inversion is over-compensating the lost frequencies resulting into a noisy output. In contrary, the sparse inversion yields a clean Q-compensation section with sparse reflectivities. It is however more difficult to assess if the Q compensation made the output reflectivity closer to the "real" one without any well information.

Finally, we show in Figure 10(a) the input data for the Australian dataset. After sparse deconvolution, we obtain Figure 10(b). Having a wavelet-free dataset, we show in Figures 10(d) and 10(c) the results of attenuation compensation with and without sparse regularization, respectively. Again, Q-compensation is improved with sparse regularization. The amplitude spectra are now shown in Figure 11(b). Here, we more clearly see the beneficial effects of attenuation compensation: improving amplitudes at late times and recovering high frequencies. Without regularization, we get the usual noisy output with a dramatic increase of the high frequencies.

6 DISCUSSION

We present a time domain method to compensate for the effect of Q in seismic data. We start with a model for spectral decay from which we extract minimum-phase Futterman wavelets using spectral factorization. With these wavelets, we form matrices representing the non-stationary time convolution with the Futterman wavelets. We then use these matrices to remove the effect of Q on the data with inversion. Because the inverse of an exponentially decaying function can become unstable, we stabilize the inversion with a regularization term that enforces sparse models. For this goal, we use the hyperbolic penalty function that can be efficiently minimized with a conjugate direction solver.

On synthetic traces, where the so-called inverse crime is commited, our proposed method works: sparse inversion yields clean and spiky reflectivity series in the presence of noise or when the wrong Q value is used for the inversion. On the contrary, inversion without regularization tends to give noisy output. On field data, where a simple constant Q model might not be appropriate, the sparse inversion also helps.

There are many shortcomings in our approach. First, we assume that Q is constant and that Q is known. We could accomodate a time-varying Q pretty easily but we don't have a good way to estimate Q from our model. Second, our view of the model is that the Q-compensated data should be sparse, which might not be the best model for all circumstances. Sparse inversion can be quite hard to tune as well and simpler regularization schemes might work just as well. Finally, our attenuation model with the Futterman wavelets might not be the best: it is a useful, simple, model giving us good insights on potential effects of Q but one that might not represent accurately enough what is observed in the data.

7 CONCLUSION

We achieve Q-compensation in the time domain by inverting matrices made of Futterman wavelets. To stabilize the inversion (i.e., avoiding exponential increases of amplitudes), we add a sparseness constraint to the inversion with the hyperbolic penalty function. The sparseness constraint makes the inversion quite robust to modeling inadequacies and noise in the data and yields spiky reflectivity series. Our model could incorporte a time-varying Q quite easily. However, finding Q remains challenging.

REFERENCES

Claerbout, J., and S. Fomel, 2014, Geophysical Imake Estimation by Example: http://sepwww.stanford.edu/data/media/public/sep//prof/gee/booksep.pdf.

Hale, D., 1981, An inverse-Q filter: SEP report, **26**, 231–243.

Sabbione, J. I., and D. Velis, 2010, Automatic first-breaks picking: New strategies and algorithms: Geophysics, **75**, V67–V76.

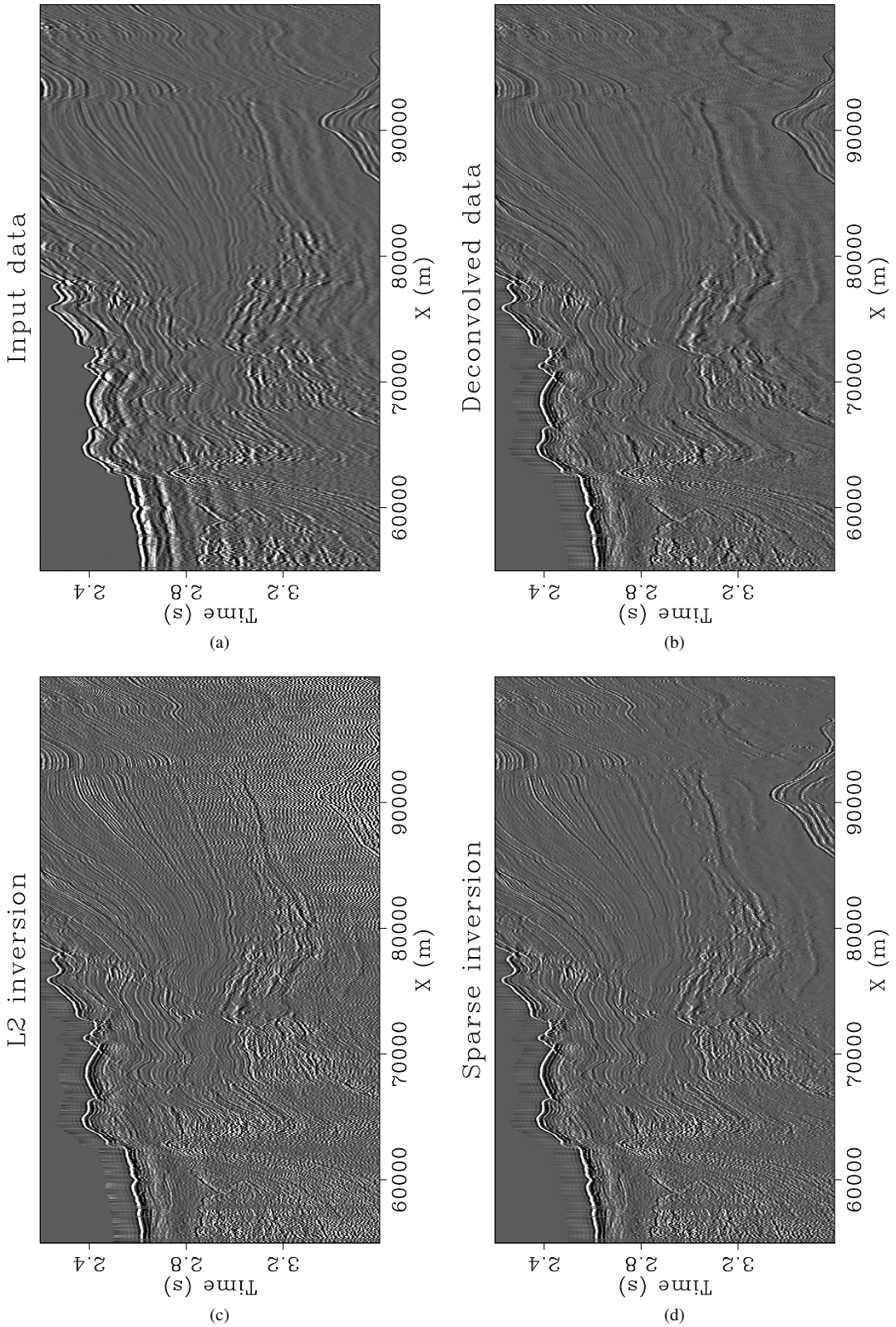

Figure 9. A near-offset section from offshore Brazil. (a) Input data with geometrical spreading correction applied. (b) Same as (a) but after sparse deconvolution. (c) Q-compensation result (Q=80) using inversion without regularization. (d) Q-compensation result with sparse inversion.

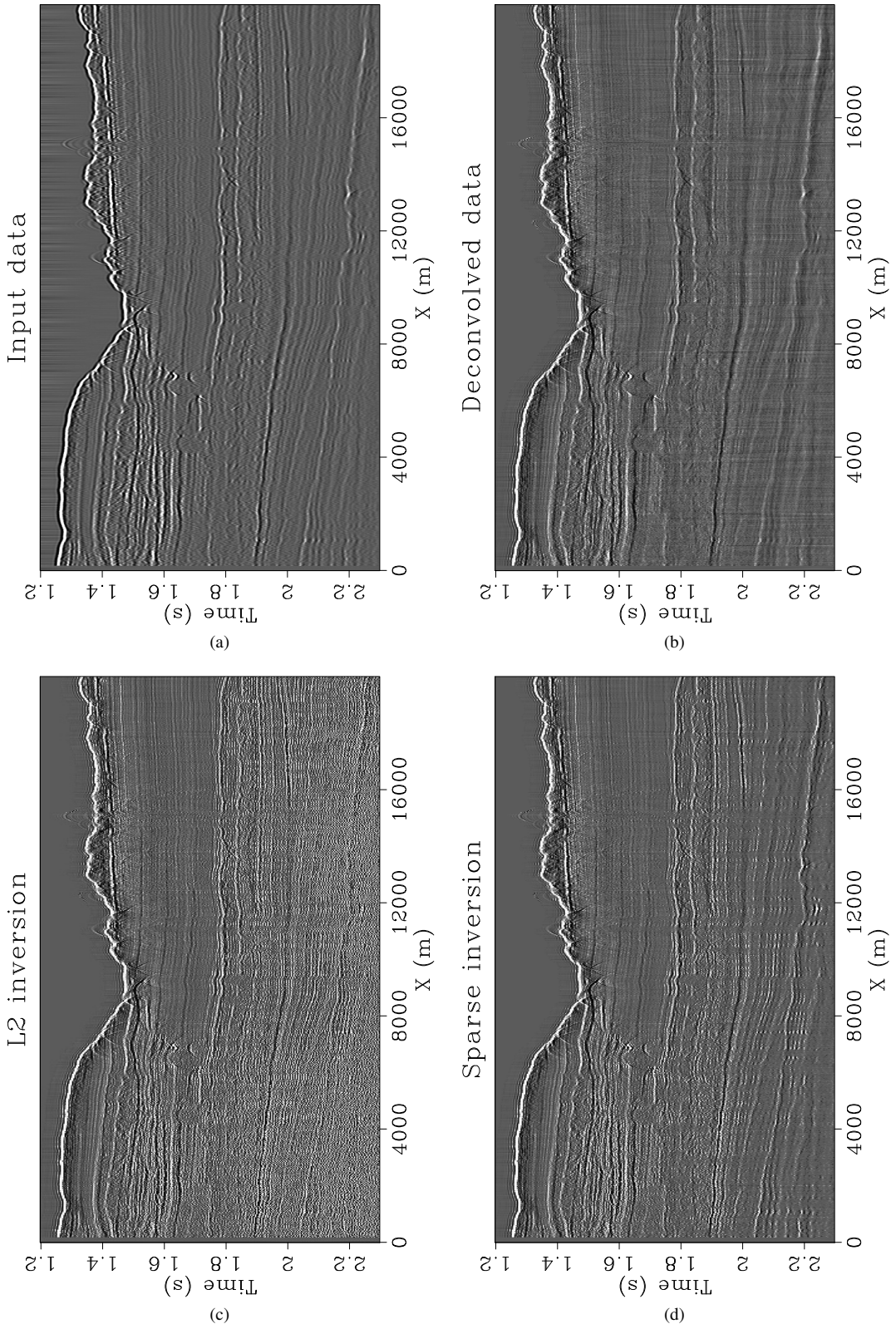

Figure 10. A near-offset section from offshore Australia. (a) Input data with geometrical spreading correction applied. (b) Same as (a) but after sparse deconvolution. (c) Q-compensation result (Q=80) using inversion without regularization. (d) Q-compensation result with sparse inversion.

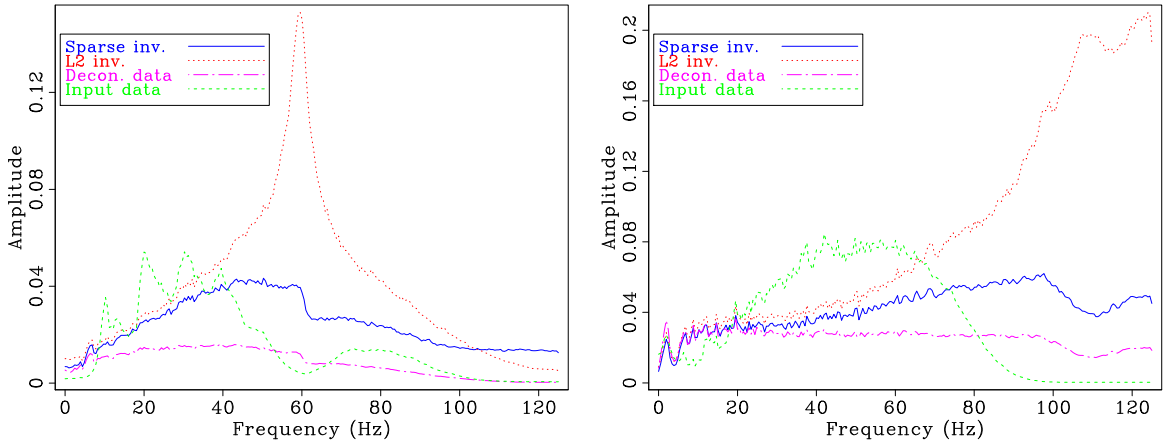

Figure 11. Amplitude spectra for the data from offshore (a) Brazil and (b) Australia. Note the huge boost of energy in the Q-compensated result at 60 Hz in (a). Without regularization, the inversion is over-compensating for the spectral hole seen in the input data.